

Band-Gap Structure of Waveguide Arrays and Excitation of Floquet-Bloch Solitons

D. Mandelik, H. S. Eisenberg, and Y. Silberberg

Department of Physics of Complex Systems, The Weizmann Institute of Science, 76100 Rehovot, Israel

R. Morandotti and J. S. Aitchison

Edward S. Rogers Sr. Department of Electrical and Computer Engineering, University of Toronto, Toronto, Ontario, Canada M5S 3G4

(Received 13 August 2002; published 6 February 2003)

Band-gap structure of periodic waveguide arrays is investigated in the linear and the nonlinear regimes. Excitation of array modes belonging to high bands is demonstrated. *Floquet-Bloch solitons* are demonstrated experimentally and shown to be a generalization of discrete solitons.

DOI: 10.1103/PhysRevLett.90.053902

PACS numbers: 42.25.Fx, 42.65.Tg, 42.65.Wi, 42.82.Et

Nonlinear effects in waveguide arrays have been studied intensively in the past several years, both theoretically [1] and experimentally [2](see also Refs. [3,4], and references therein). Most of the work was concentrated on discrete solitons, which are usually analyzed in the framework of the coupled-mode theory, using the discrete nonlinear Schrödinger equation (DNLSE) [1]. In this framework, the array mode is described as a collective excitation (a “supermode”) of the individual waveguides’ modes, evanescently coupled to each other. The supermode is described in terms of the individual modes’ complex amplitudes, with the details of the field between the waveguides packed up into a single parameter—the coupling constant, which enters the DNLSE.

This approach, although intuitive, suffers from a lack of generality. A more general approach, in which waveguide arrays are regarded as an example of a general one-dimensional periodic optical structure, is the Floquet-Bloch (FB) analysis. It predicts that the propagation-constant spectrum of the array’s eigenmodes (the FB waves) is divided into bands, separated by gaps in which propagating modes do not exist [5,6]. Figure 1 shows the calculated diffraction relation (band-gap diagram) of a typical waveguide array. It relates the propagation constant β to the Bloch wave number, K , which is the transverse component of the wave vector reduced to the first Brillouin zone. The propagation direction of each mode is given by the normal to the diffraction curve. The coupled-mode analysis describes only propagation within the first of these bands, where the energy is concentrated in the high-index waveguides. The diffraction curve of this first band is nearly sinusoidal, as predicted by the coupled-mode theory. For reasons that are discussed below, the geometry in which all previous experiments were performed favors the excitation of the first band, which is another reason for the success of the coupled-mode approach. Although the coupled-mode analysis was extended to describe the second band [7], it seems that a different approach should be taken, in order to generally describe excitations in higher bands. The purpose of this work is to investigate the band structure of waveguide

arrays and to realize linear and nonlinear propagation in higher bands. The Floquet-Bloch approach is used as the theoretical basis for the analysis of our experimental observations, both in the linear and the nonlinear regimes. We note that the general problem of propagation in periodic media has been attracting significant attention recently, in connection with the recent advance in photonic band-gap materials [8], and more specifically in the context of gap solitons [9]. Our work therefore connects the recent works on discrete solitons and waveguide arrays with those on photonic band-gap structures.

To excite a single FB mode in a waveguide array, we use the geometry illustrated in the inset of Fig. 2, where a beam is coupled at a grazing angle to the array from a region of a planar waveguide (i.e., the continuum) along its side. A pure FB mode is excited, with a propagation constant β , which is matched to k_z , the z component of the k vector in the continuum [6]. Any specific {band No., K } combination, K being the Bloch wave number, may be excited by tilting the input beam to the required angle.

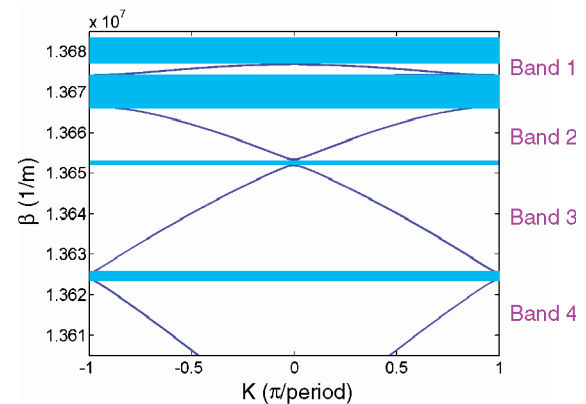


FIG. 1 (color online). Reduced band-gap diagram of a typical waveguide array (i.e., folded into the first Brillouin zone), where the propagation constant is plotted as a function of the Bloch wave number. The shaded regions represent the gaps. The four lowest lying bands (highest propagation constants) are shown.

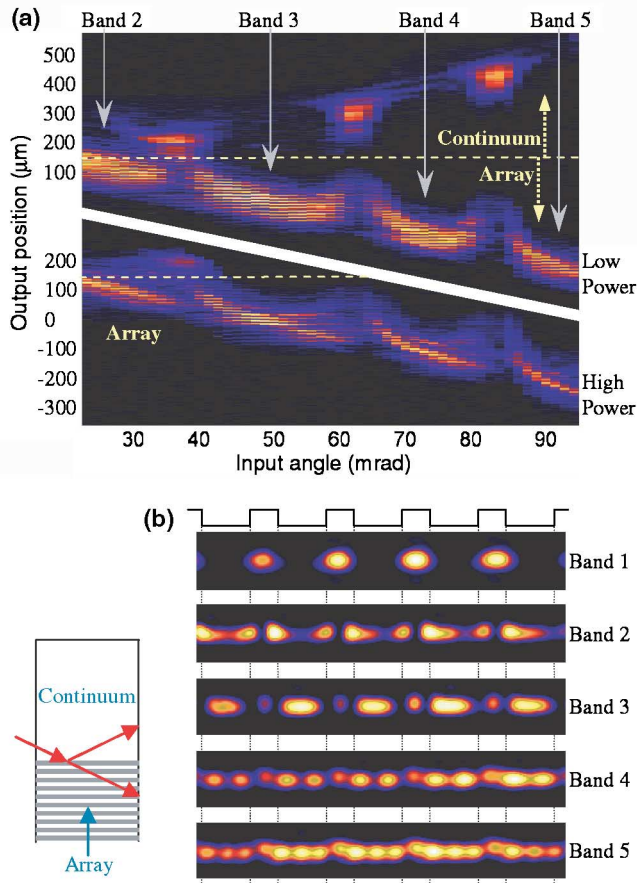


FIG. 2 (color online). Pure FB-wave excitation using the geometry shown in the inset. (a) Cross sections of the measured intensity distribution at the sample output as a function of the input-beam angle, at low (upper panel) and high (lower-panel) input powers. The high-power measurement was conducted at approximately 2 kW peak power. (b) Highly magnified images of the pure FB modes excited in each band at low powers. The high-power excitation reproduced the same modal shapes.

Figure 2 shows typical results of such a measurement. In Fig. 2(a), cross sections of the intensity distribution at the array output are plotted as a function of the input-beam angle. The experimental setup was identical to that described in Ref. [2]. The waveguide's width was $4 \mu\text{m}$, the array period was $11 \mu\text{m}$, and the refractive-index step was 0.007 (about 3–6 times larger than those used in previous experiments [2]). A wide input beam (about $70 \mu\text{m}$ FWHM) was used, to define a narrow spectral content of the excitation. The band-gap structure of the array is clearly demonstrated in the low power results, shown in the upper panel of Fig. 2(a). For angles that match the band gaps the beam is reflected almost totally from the array interface, back into the continuum region. Between the gaps, the beam excites pure FB modes. Note that in each band there is an angle of incidence that leads to maximum penetration into the array, which corresponds to the steepest point in the diffraction curve for that band. Figure 2(b) shows a photograph of the

modal intensity distribution at the array output for each band. Clearly, the FB modes belonging to higher bands have much of their energy distributed in the lower index regions between the waveguides, with an increasing number of oscillations. The intensity distribution of band No. 1 was measured using head-on excitation, as described below, since the continuum part of our samples was etched down, limiting from above the range of available β 's.

Figure 2(a) also shows, in the lower panel, the results of a high-power experiment, using identical conditions to that of the low-power experiment. Two important observations call for a discussion. First, there is a clear change in the band curvature (i.e., the penetration of the beam into the array, plotted as a function of the input angle), suggesting an intensity dependent modification of the diffraction curves. Nevertheless, the band-gap structure remains essentially unchanged, even at powers high enough to cause self-focusing of the beam into a soliton and beyond, reaching soliton-breakup powers.

Second, the excited FB modes retain their characteristic modal shapes even at the highest powers. Beam propagation analysis was conducted [10], which simulates the measurement shown in Fig. 2. Results are illustrated in Fig. 3(a), which shows the intensity distribution of the beam at the array output, after traveling across the array in a band No. 4 mode, at low and high power. At low power, the beam diffracts as expected, into a wide output beam (a narrow input beam is used, $8 \mu\text{m}$ FWHM width, to emphasize the diffraction of the linear FB mode). At a high power, the FB mode stabilizes (while shedding part of its power) into a bright narrow soliton, as seen in Fig. 3(a). It is clear from Fig. 3(a) that the modal shape of the soliton matches that of the pure (linear) band No. 4 FB mode, in all its details: a single peak in a waveguide and two peaks between waveguides, as in Fig. 2(b). Thus, launching of a FB mode in this way at sufficiently high power leads to the formation of a *Floquet-Bloch soliton*, propagating across the array without changing its envelope width or its internal modal shape. Thus, such a FB soliton can be expanded in terms of FB waves, all belonging to a single band.

These FB solitons have been studied theoretically in band No. 2 [7], where the DNLSE is modified so that it includes the second lying band in the FB spectrum. Temporal FB solitons have been studied in the context of gap solitons, using normal propagation inside a layers-stack structure (e.g., Bragg-grating fibers) [9]. A more general approach is taken in Ref. [11] (see also references therein). The author uses a reductive perturbation method to show that the envelope of a nonlinear FB wave may be described by the nonlinear Schrödinger equation (NLSE), yielding, under specific conditions, bright and dark soliton solutions. Discrete solitons may therefore be regarded as a particular member of the FB-solitons family, those belonging to the first band. We believe that such FB solitons were excited in all bands in our high-power

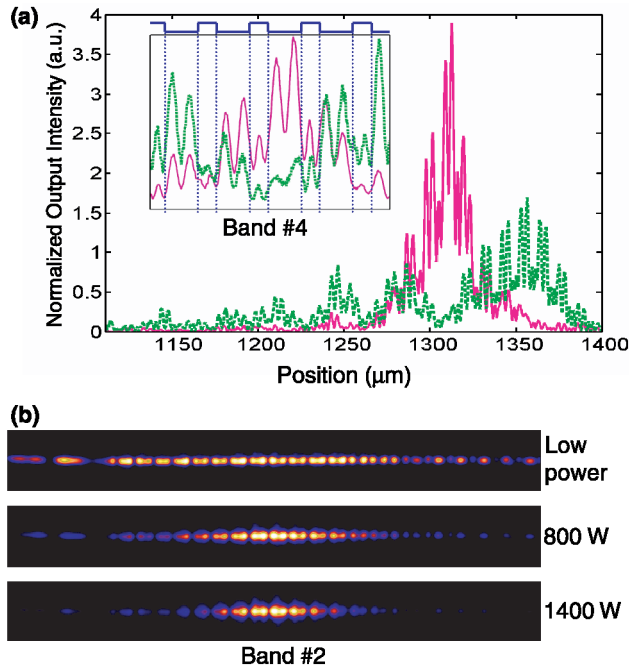


FIG. 3 (color online). (a) Beam propagation simulation simulation results of the measurement described in Fig. 2, showing the beam at the array output, for low power (dotted line) and high power (solid line). The inset shows a magnified section of the plot, demonstrating the identical modal shapes of the low-power (diffracting) beam and the band No. 4 FB soliton formed at high power. (b) Photograph of the intensity distribution at the array output of a band No. 2 FB mode, at low, intermediate, and high output power (approximate peak powers are indicated). At low power, the input beam weakly excites band No. 3 (right side of the figure), and diffracts partly into the continuum (left side of the figure). At high power, a band No. 2 FB soliton is formed.

experiment, shown in Fig. 2. The high-power measurement was repeated using a narrow beam [similar to the one used in the simulations shown in Fig. 3(a)], yielding a clear observation of the formation of a bright soliton. Typical results are given in Fig. 3(b), which shows photographs of the intensity distribution at the array output. At low power, the beam excites a diffracting band No. 2 mode. As power increases the distribution narrows, until a band No. 2 FB soliton is formed.

The existence of FB solitons and their properties depend on the Bloch wave number K around which they are centered. This is well understood when considering the calculated diffraction values of the FB modes, shown in Fig. 4(a). It is clearly seen that the diffraction sign and magnitude vary significantly within each band, thus causing different behavior of the FB soliton at different Bloch wave numbers across each band. This is further emphasized in the experimental results shown in Fig. 4(b), where cross sections of the intensity at the array output are plotted as a function of the output power for two points in band No. 4, as marked in (a). In point 1 where

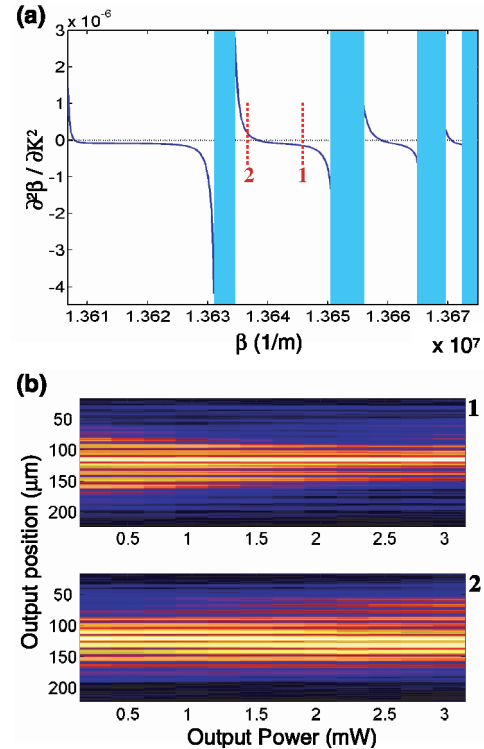


FIG. 4 (color online). (a) Theoretically calculated diffraction of a typical array, plotted as a function of the propagation constant. The shaded areas represent the gaps. Bands 2 to 5 are seen, from right to left. Band 1, with the largest propagation constant, is not visible in this scale. (b) Measurement results of the intensity distribution at the array output, plotted as a function of the average output power, for the points indicated in the diffraction plot of part (a).

the diffraction is normal (negative) the beam focuses into a bright FB soliton. In contrast, the beam in point 2 does not exhibit any focusing, due to the anomalous diffraction of band No. 4 at that point. This type of behavior has been observed before in discrete solitons [12], leading to non-linear defocusing and discrete dark solitons in the anomalous diffraction regime of band No. 1, which extends over half of that band. We note, however, that at higher bands the region of anomalous diffraction shrinks due to the band curvature.

The geometry described above is the only way to achieve pure FB-mode excitation. The geometry most widely used in experiments, however, is the head-on excitation shown in the inset of Fig. 5. In this geometry, all the {band No., K } combinations having their Bloch wave number K equal to k_x , the x component of the continuum k vector, will be excited [6]. Thus, in this geometry it is impossible to excite a pure FB wave in the array. Instead, a set of FB waves will be excited, each one traveling at a different direction in the array (given by the normal to the diffraction curve), and with their relative amplitudes determined by their overlap with the beam profile at the array input. At a low index step

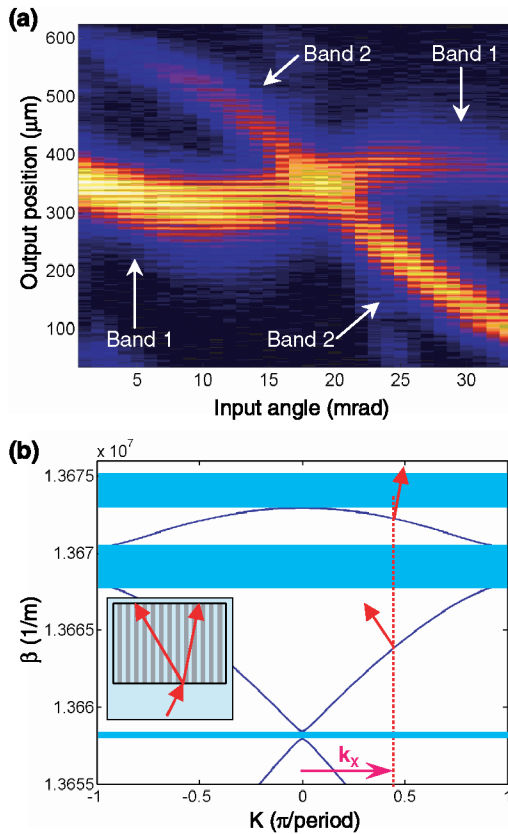


FIG. 5 (color online). Measurement results for the case of a mixed excitation of two FB waves using the geometry shown in the inset. (a) Cross sections of the intensity distribution at the array output as a function of the input-beam angle. (b) Theoretically calculated band-gap diagram of the measured array, showing the two lowest-lying bands (highest β 's), and indicating the propagation direction of the FB modes. k_x represents the x component of the continuum k vector. The shaded regions represent the gaps.

(0.0015 or less), the overlap of the band No. 2 mode with the Gaussian beam at the input is small, due to the modal shape of the field; thus, the band No. 1 mode is primarily excited. This explains why, in low index-step samples like those used in most of the experimental work to date [3], significant high band excitation was never observed.

Figure 5(a) shows measurement results, using the geometry shown in the inset, with a $9\ \mu\text{m}$ -period array. Again, cross sections of the output intensity were taken and plotted as a function of the input-beam angle. Excitation of two FB modes is clearly seen, with the band No. 2 mode growing stronger as the beam angle is increased, until the edge of the (first) Brillouin zone is reached at an angle where $k_x = \pi/a$ (a being the array period), and the band No. 2 mode becomes the dominant excitation. The two excitations were easily distinguished by their characteristic modal shape [see Fig. 2(b)]. Higher bands were also excited (mostly band No. 3), but with a much smaller amplitude (by an order of magnitude or

more). The reason for this is that higher band modes have small overlap with the Gaussian beam at the input, due to the rapid oscillations of their modal field distribution. Generally speaking, at each input angle, two bands are primarily excited, traveling in opposite directions across the array. The higher the input angle, the higher will be the bands of this pair. Notice also the limited range of directions in which the mode No. 1 propagates, as compared to the larger range of propagation directions exhibited by the mode No. 2, all in agreement with the calculated band-gap diagram of the measured array, shown in Fig. 5(b).

In conclusion, we investigated experimentally the band structure of waveguide arrays and realized linear and nonlinear propagation in higher bands using two types of geometries. In the “side-coupling” geometry, a pure FB mode is excited, at any desirable {band No., K } combination. In the head-on geometry, two FB modes are primarily excited. The Floquet-Bloch approach was used to analyze our experimental observations, both in the linear and the nonlinear regimes. Floquet-Bloch solitons were observed, and shown to be a generalization of discrete solitons, for higher array bands.

The authors gratefully acknowledge the financial support of the U.S.-Israel Binational Science Foundation (BSF) and the Natural Science and Engineering Research Council (NSERC).

- [1] D. N. Christodoulides and R. I. Joseph, *Opt. Lett.* **13**, 794 (1988).
- [2] H. S. Eisenberg, Y. Silberberg, R. Morandotti, A. R. Boyd, and J. S. Aitchison, *Phys. Rev. Lett.* **81**, 3383 (1998).
- [3] F. Lederer and Y. Silberberg, *Opt. Photonics News* **13**, 48 (2002).
- [4] F. Lederer, S. Darmanyan, and A. Kobayakov, in *Discrete Solitons*, edited by S. Trillo and W. Torruellas (Springer-Verlag, Berlin, 2001).
- [5] P. Yeh, A. Yariv, and C. S. Hong, *J. Opt. Soc. Am.* **67**, 423 (1977).
- [6] P. St. J. Russell, *Appl. Phys. B* **39**, 231 (1986).
- [7] A. A. Sukhorukov and Y. S. Kivshar, *J. Opt. Soc. Am. B* **19**, 772 (2002).
- [8] E. Yablonovitch, *Phys. Rev. Lett.* **58**, 2059 (1987). See also J. D. Joannopoulos, R. D. Meade, and J. N. Winn, *Photonic Crystals: Molding the Flow of Light* (Princeton University, Princeton, NJ, 1995).
- [9] D. N. Christodoulides and R. I. Joseph, *Phys. Rev. Lett.* **62**, 1746 (1989). See also C. M. de Sterke, B. J. Eggleton, and J. E. Sipe, in *Spatial Solitons*, edited by S. Trillo and W. Torruellas (Springer-Verlag, Berlin, 2001).
- [10] The BPM-simulation package is available at www.FreeBPM.com
- [11] T. Iizuka and M. Wadati, *J. Phys. Soc. Jpn.* **66**, 2308 (1997).
- [12] R. Morandotti, H. S. Eisenberg, Y. Silberberg, M. Sorel, and J. S. Aitchison, *Phys. Rev. Lett.* **86**, 3296 (2001).